Directed self-assembly of CdS quantum dots on bacteriophage P22 coat protein templates

2013 Nanotechnology 24 045603

(http://iopscience.iop.org/0957-4484/24/4/045603)

Nanotechnology **24** (2013) 045603 (6pp) doi:10.1088/0957-4484/24/4/045603

Directed self-assembly of CdS quantum dots on bacteriophage P22 coat protein templates

Anup Kale[1], Yuping Bao[2], Ziyou Zhou[2], Peter E Prevelige[3] and Arunava Gupta[1,4]

[1] Centre for Materials for Information Technology, The University of Alabama, Tuscaloosa - 35487, AL, USA
[2] Department of Chemical and Biological Engineering, The University of Alabama, Tuscaloosa, AL, 35487, USA
[3] Department of Microbiology, University of Alabama at Birmingham, Birmingham - 35294, AL, USA

E-mail: anupakale@gmail.com, prevelig@uab.edu and agupta@mint.ua.edu

Received 24 July 2012, in final form 6 November 2012
Published 7 January 2013
Online at stacks.iop.org/Nano/24/045603

Abstract
The hierarchical organization of inorganic nanostructures has potential applications in diverse areas such as photocatalytic systems, composites, drug delivery and biomedicine. An attractive approach for this purpose is the use of biological organisms as templates since they often possess highly ordered arrays of protein molecules that can be genetically engineered for specific binding. Indeed, recent studies have shown that viruses can be used as versatile templates for the assembly of a variety of nanostructured materials because of their unique structural and chemical diversity. These highly ordered protein templates can be employed or adapted for specific binding interactions. Herein we report the directed self-assembly of independently synthesized 5 nm CdS nanocrystal quantum dots on ~60 nm procapsid shells derived from wild-type P22 bacteriophage. The bacteriophage P22 shell is comprised of hexameric and pentameric clusters of subunits known as capsomeres. The pre-synthesized CdS QDs show the corresponding hexameric and pentameric patterns of assembly on these P22 shells, possibly by interacting with particular protein pockets.

S Online supplementary data available from stacks.iop.org/Nano/24/045603/mmedia

(Some figures may appear in colour only in the online journal)

1. Introduction

Viruses have emerged as effective scaffolds for use in nano-medicine and materials synthesis because of their unique functional and structural properties. Over the past decade there have been significant advances in the use of a variety of engineered viruses, such as M13, HK97, phi29, P22, etc, for the synthesis and assembly of nanostructured inorganic materials [1–12]. This has been possible in large part because of the improved understanding of the structure, assembly and maturation of these viruses. Hierarchical assembly of nanostructured materials using virus templates has drawn considerable attention for potential applications in diverse areas such as photocatalytic systems, composites, drug delivery, and biomedicine [1, 6, 7]. The unique advantage of these virus particles is that they can be genetically and chemically manipulated and explored as nano-templates at three levels of their structure, namely their outside surface, inside surface and at the interface between the subunits [4]. Moreover, these biotemplates can be crucial for the synthesis of nanomaterials that are difficult to obtain by traditional chemical routes. Whereas the focus thus far has primarily been on the use of these versatile templates for the synthesis of a variety of nanocrystals ranging from metals to

[4] Author to whom any correspondence should be addressed.

semiconductors, the interactions of these versatile templates with pre-synthesized nanocrystals and their potential as templates for the assembly of nanocrystals have been much less studied.

Bacteriophage P22 is a robust spherical nano-template with unique structural and functional capabilities. The organization of and maturation of procapsids of icosahedral viruses such as P22 is reasonably well understood [13]. Besides the use of engineered phages for materials synthesis via controlled nucleation and growth using suitable chemical precursors, it is of interest to understand the natural interaction between surfactant-capped quantum dots with the cage proteins. This would expand the utility of these templates for wider applications in materials and biological sciences. In this paper we report on the ordered assembly of independently synthesized CdS quantum dots (QDs) on the coat protein shells of wild-type P22. The CdS QDs are observed to assemble in ordered arrays of mostly hexagonal and pentagonal patterns, apparently due to their binding affinity at specific coat protein pockets.

2. Materials and methods

2.1. Preparation and purification of wild-type bacteriophage P22 procapsid shells

Wild-type procapsid shells were obtained by co-expression of coat protein and scaffolding protein in *E. coli* (BL21 DE3) at 37 °C. Procapsids were purified from cell pellets using a protocol that has been described previously [14]. Briefly, 1 mM isopropyl β-D-1-thiogalactopyranoside (IPTG) induced *E. coli* cells were harvested by centrifugation and lysed by repeated freeze-thaw cycles in Lysis Buffer (50 mM Tris, 100 mM NaCl, 5 mM $MgSO_4$, pH 7.6). The lysate was centrifuged at 10,000 rpm (SW34 Beckman Rotor) for 45 min at 4 °C and the supernatant containing the procapsids was then centrifuged in 20% sucrose solution (20% Sucrose, 50 mM Tris, 100 mM NaCl, 5 mM Mg_2SO_4, pH 7.6) at 40,000 rpm (42.1 Beckman Rotor) for 1 h to pellet the procapsids. The scaffolding protein was extracted from the procapsids using 0.5 M GuHCl (guanidine hydrochloride) in buffer B (25 mM Tris-HCl, 25 mM NaCl, 2 mM EDTA, pH 7.6). The extraction step was repeated twice. The coat protein shells were separated from the scaffolding protein on a sucrose gradient (5–20%) containing 0.5 M GuHCl in buffer B (SW41 Beckman Rotor). The shells were collected by centrifugation at 38,000 rpm (42.1 Beckman Rotor) for 1 h at 4 °C and resuspended in buffer B and stored at 4 °C.

2.2. Ligand exchange-based phase transfer of CdS quantum dots from organic to aqueous phase

Oleic acid-capped CdS quantum dots (QDs) with average diameter of 5 nm in toluene were purchased from NN-Labs LLC, AR, USA. The ligand exchange reaction was carried out as reported by Wei *et al* [15]. First, 300 mg (1 mmol) of glutathione (GSH) and 540 mg (3 mmol) of tetramethylammonium hydroxide pentahydrate (TMAH) were dissolved in 10 ml of methanol to form the GTMA salt (100 mM). Next, 1 ml of toluene solution of CdS QDs was dissolved in 5 ml of chloroform. Subsequently, 1.0 ml of GTMA solution was added dropwise to the CdS QD solution in the organic phase with rapid and continuous stirring. The QD nanoparticles first precipitated due to ligand exchange of the oleic acid for GTMA. Then some additional GTMA solution was added to dissolve the precipitate. Stirring was continued and as a final step 5.0 ml of water was added to the mixture. The mixture was left to stand for a couple of hours and the upper aqueous phase with negatively charged CdS QDs was collected without disturbing the mixture (please refer to supporting information SI1 and SI2 available at stacks.iop.org/Nano/24/045603/mmedia). The nanoparticles solution was then dialysed (3000 molecular weight dialysis membrane) overnight against deionized water to remove the unreacted surfactant. The aqueous sample was stored at 4 °C until used.

2.3. Interaction of CdS QDs with P22 shells

The wild-type bacteriophage P22 shells after purification were 4000× dialysed against deionized water for 16–18 h with three changes of water. These P22 shells were then used as biotemplates for the assembly of CdS QDs. 10 μl of P22 shells solution was added to 1 ml of the solvent at 25 °C and allowed to stabilize for 10 min. Then 10 μl of purified CdS QDs solution was added to it, mixed by gentle inversion for 10 s. The reaction mixture was kept in a thermo-mixer at 250 rpm operated at 25 °C for up to 24 h. The protein concentration in the reaction mixture was 25–50 μg and corresponding CdS QDs concentration was adjusted so as to obtain a ratio of 500:1 for CdS QDs per P22 procapsid shell.

2.4. Transmission electron microscopy experiments

Scanning transmission electron microscopy (STEM) and transmission electron microscopy (TEM) examinations were performed using a FEI Tecnai F-20 electron microscope operated at 120/200 keV, equipped with a Gatan CCD camera for image capture. The 300 mesh formvar coated copper grids, stabilized with evaporated carbon (Electron Microscopy Sciences, Hatfield, PA) were used to prepare the samples. 10 μl of the sample, i.e. purified P22 procapsid shells or after the self-assembly of CdS QDs, was placed on the grid and observed under the electron microscope for the morphology, structure and assembly of the QDs and procapsid shells. In case of only P22 procapsid shells, the samples were negatively stained with 2% uranyl acetate, blotted and allowed to air dry. In the case of samples with quantum dots, examinations were performed without staining. While observing the samples for P22 shells and CdS QDs bound P22 shells, the electron microscope was operated at 120 keV to ensure that the proteins were not damaged by the electron beam and for samples with only CdS QDs and uranyl acetate stained samples, the electron microscope was operated at 200 keV.

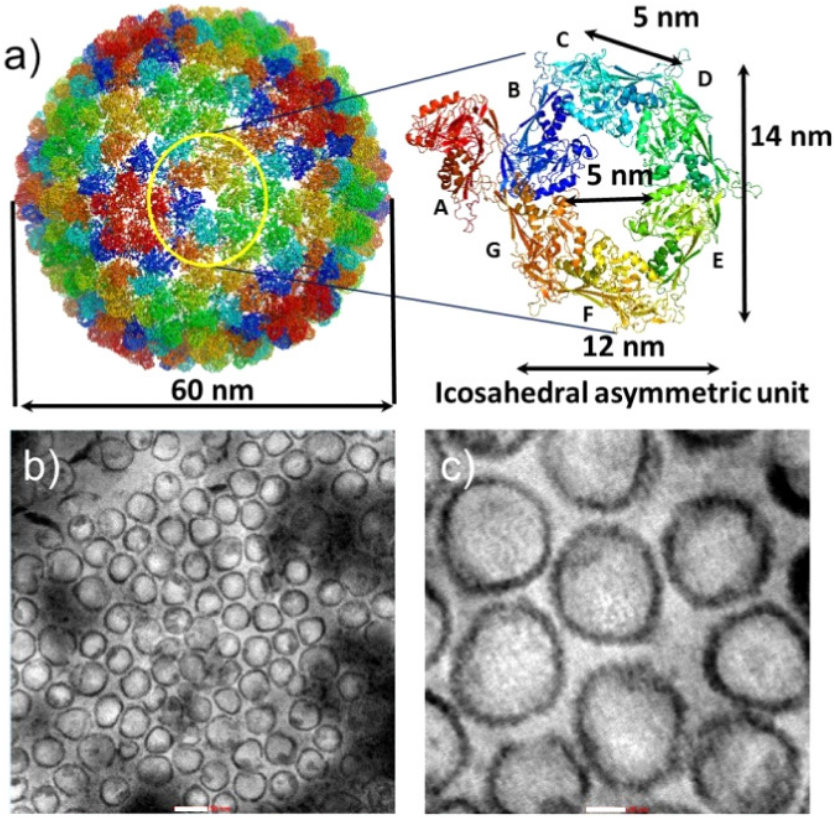

Figure 1. (a) P22 coat protein shell showing the assembly of 420 coat proteins and one icosahedral asymmetric unit holds one whole hexon (B through G subunits) and one penton subunit (A subunit). (b, c) Transmission Electron Microscopy (TEM) images of wild-type P22 shells obtained after staining. Scale bar in (b) is 50 nm and in (c) is 20 nm.

2.5. Dynamic light scattering and fluorescence spectroscopy measurements

The hydrodynamic size of CdS QDs, procapsid shells and CdS QDs-assembled procapsid shells in aqueous solution were measured using dynamic light scattering (DLS) analysis (Zetasizer Nano, Malvern). The fluorescence measurements on the samples were performed using a Cary Eclipse fluorescence spectrophotometer.

3. Results and discussion

The protein shell of P22 has icosahedral symmetry and is assembled from 420 subunits of coat proteins. These are organized as 60 asymmetric units, each consisting of 7 coat protein subunits [13]. Figure 1(a) depicts the 60 nm procapsid shell along with a single icosahedral asymmetric unit containing a complete hexon (B through G subunits) and a penton subunit (A subunit). The wild-type (WT) P22 shells for the experiments were prepared by extraction of the scaffolding proteins from the procapsids. Figures 1(b) and (c) show TEM images of P22 wild-type shells obtained after staining. Monodisperse CdS quantum dots (QDs) of 5 $\pm$ 1.2 nm size were studied for binding onto the coat protein shells. Prior to the binding studies, the hydrophobic oleic acid cap on the CdS QDs was exchanged for a hydrophilic carboxylate cap using gluathione tetramethylammonium salt (GTMA) as the ligand. These negatively charged CdS QDs were mixed with 4 μM of wild-type P22 procapsid shells in deionized water at 40 °C for up to 24 h for the binding studies.

Figure 2(a) shows TEM images of CdS QDs obtained after 4 h of incubation. The nanoparticles appear to display hexagonal and pentagonal patterns of binding on the surface of ~60 nm P22 shells. When the incubation time was prolonged to 24 h, the assembly pattern of CdS QDs remained essentially unchanged. This suggests that the binding process is sufficiently rapid to be completed within the initial time period (also see supporting information SI3 available at stacks.iop.org/Nano/24/045603/mmedia). To assess the effect of electrostatics on binding we performed experiments at both pH 4 and pH 9. The isoelectric point (pI) of P22 is 4.97 [16], so at pH 4 it will carry almost equal positive and negative charges. Interestingly, at this acidic pH, the hexameric and pentameric capsomeres appear to pop out of the shells, disturbing the shell structure. Even though the shell structure is disturbed, the CdS NPs still show binding to the popped-out hexamers and pentamers in the TEM images (see supporting information SI4 available at stacks.iop.org/Nano/24/045603/mmedia). In many of the capsomeres, the specific hexameric and pentameric assembly patterns of CdS NPs can be observed, as seen in the interaction with intact shells. These observations indicate the specificity of the binding of coat proteins domains with CdS NPs. At highly basic pH, around 9, neither P22 shells nor the CdS QDs are stable.

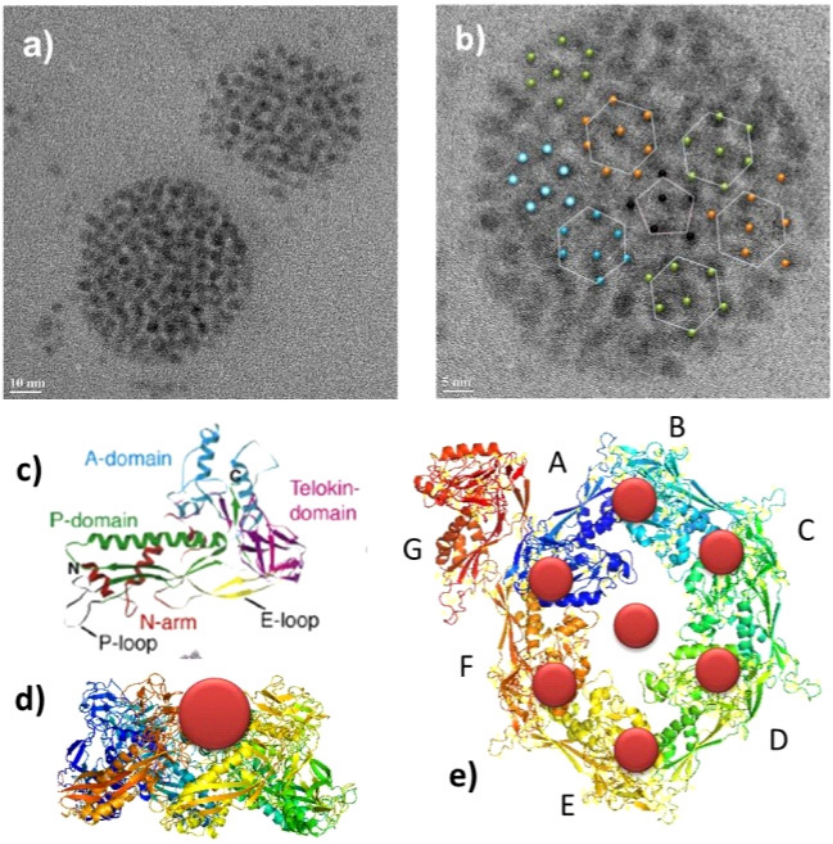

Figure 2. (a) Transmission electron microscopy (TEM) images showing assembly of 5 nm CdS nanoparticles on wild-type P22 shells. Scale bar is 10 nm. (b) TEM micrograph depicting the hexameric and pentameric patterns of assembly of CdS nanoparticles on a single P22 shell (also refer supporting information SI6 available at stacks.iop.org/Nano/24/045603/mmedia). Orange, green, and blue dots indicate the individual hexamers and black dots indicate pentamers. Scale bar is 5 nm. (c) A single P22 coat protein showing the projection of different domains (reproduced with permission from [19]). (d) Lateral view and (e) top view of a single asymmetric unit with red dots showing one possible CdS binding site on a hexamer.

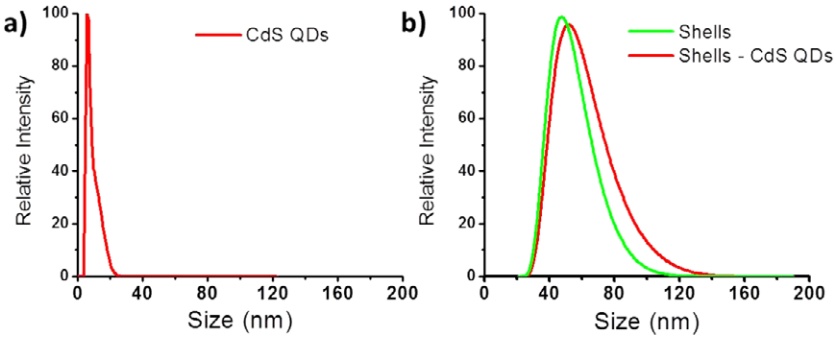

Figure 3. Dynamic light scattering (DLS) measurements of (a) CdS QDs (mean size 5.0 ± 1.2 nm); (b) shells (mean size 50.8 ± 10.0 nm) and CdS QDs assembled on shells (mean size 56.2 ± 12 nm). Note that the data is presented as relative intensity measurements.

We have further studied the assembly process by dynamic light scattering (DLS, Zetasizer Nano S series, Malvern Instruments). The mean size of the CdS QDs in aqueous solution is determined to be 5.0 ± 1.2 nm (figure 3(a)). DLS provides the hydrodynamic size, which is somewhat larger than that obtained from TEM images, possibly because of the contribution of the electrical double layer around the nanoparticle. A similar measurement of an aqueous suspension of the P22 shells provides a size distribution of 50.8 ± 10.0 nm (figure 3(b), green line). As would be expected, a shift of the distribution to a higher mean value is observed after interaction of the CdS QDs with the P22 shells (figure 3(b), red line). The QD–shell assembly shows a single distribution with a mean size of 56.2 ± 12 nm, indicating that they form a stable dispersion, as seen in figure 3(b).

The fluorescence spectra, before and after binding of the CdS QDs on the shells, have been recorded in order to ascertain changes in the interaction (figure 4(a)). The

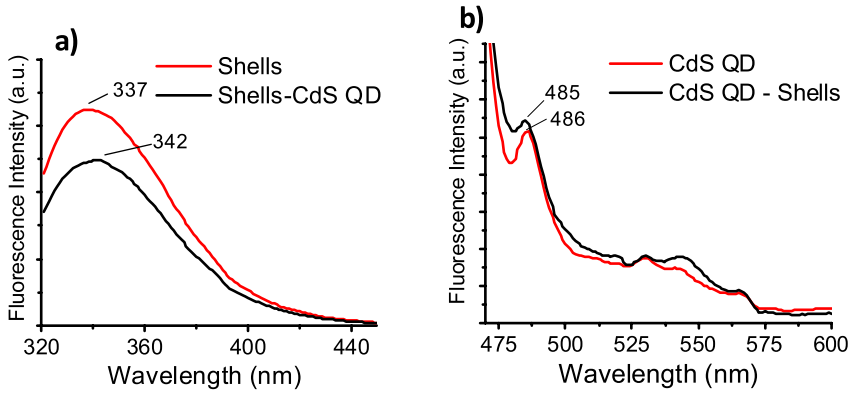

Figure 4. Fluorescence spectra of (a) shells alone and shells after binding with CdS quantum dots ($\lambda_{ex} = 280$ nm); (b) fluorescence spectra of CdS quantum dots alone and after binding with shells ($\lambda_{ex} = 460$ nm).

fluorescence spectrum of the shells after interacting with the quantum dots undergoes a bathochromic shift by about 7 nm as compared to the shells alone. This suggests formation of a complex between the shells and CdS QDs. Formation of the complex likely results from electrostatic interaction of the coat proteins with the nanoparticles forming a layer on the surface of the shells. In contrast, there is no significant shift in the fluorescence spectrum of the CdS QDs with 460 nm excitation (figure 4(b)). A likely reason for the decrease in the intensity and slight shift in the fluorescence peak of the P22 shells bound to CdS QDs is partial charge transfer from the CdS QDs to the protein ligands. Because of the strong interaction between adjoining proteins, a change in their geometry because of interaction with the QDs is unlikely to cause any noticeable shift in the fluorescence spectra.

Based on the TEM images in figure 2, the distance between two oppositely positioned CdS QDs in the hexagonal assembly is estimated to be ∼13–15 nm, while that between two neighbouring CdS QDs is ∼4–6 nm. As mentioned earlier, P22 has an isometric structure comprised of 420 subunits forming 72 capsomers, 60 of which are hexameric oligomers (hexamer) and 12 are pentameric oligomers (pentamer) [17, 18]. The measured distances between the assembled QDs correlate well with the known spacings of the proposed binding domains of coat protein in the hexamers and pentamers (PDB entry 3IYI). The distance between two opposite vertices of the hexamer is about 14 nm and the distance between to opposite P-domains is about 10 nm, with the distance between two adjacent P-domains or ED domains being ∼5 nm (figure 1(c), also see SI4 available at stacks.iop.org/Nano/24/045603/mmedia). If one nanoparticle binds to each subunit, with 420 copies of coat proteins, and one nanoparticle outside, at the centre of the each hexamer (60), the total number of nanoparticles would be 480 (420 + 60).

We have performed zeta potential measurements (Zetasizer Nano, Malvern) on the P22 shells and the CdS quantum dots, and the results are shown in the supporting information (SI5) (available at stacks.iop.org/Nano/24/045603/mmedia). As seen from the data, both the P22 shells and the QDs are overall negatively charged, with sufficiently high zeta potential values to explain their colloidal stability (>±30 mV). Negative zeta potential values for bacteriophages have been previously reported [19], and a negative value for the QDs is expected because of the presence of the negatively charged carboxylate ligands. To explain the observed ordered assembly, we propose that the QDs bind to P22 shells at specific positively charged coat protein pockets notwithstanding the overall negative charge. Examining the details of the structure and organization of the P22 procapsids provides some insight regarding the CdS assembly patterns. For the 46.6 kDa P22 coat protein, the unit structure of the shell preserves a HK97-like core structure that contains four α helices (H0–H3), β sheets and different domains, namely N-arm, P-loop, P-domain, E-loop, A-domain and telokin domain (figure 2(c)) [20–24]. The P-domain has a core H1 helix. The structural details of the P22 shells suggest that CdS QDs can possibly interact with a protruding region such as the telokin domain, or alternatively nestle in a preformed pocket such as the one between subunits. Both these sites are significantly polar and have lysine residues, which can act as positively charged ligands favouring electrostatic interaction [25]. Apart from these sites, the other domains are primarily involved in the subunit interactions and stability of the procapsid shell. In both the procapsid and mature states the inner coat protein domain extends underneath the outer domain of the adjacent subunit and towards the local three-fold axes, forming extensive interactions with equivalent subunits of the adjacent three hexamers.

4. Conclusions

The results of our study clearly demonstrate that wild-type P22 shells can be used as a template for the ordered assembly of preformed CdS nanocrystals. Details of the CdS QD—P22 protein interaction sites are not yet understood, but we have proposed some possible coat protein pockets for binding affinity. Selective electrostatic interaction of inorganic nanomaterials with protein sites is quite common and the demonstrated scheme can thus be exploited for use with other inorganic materials and on a variety of other biological templates. The ordered inorganic nanostructures fabricated by this simple approach can be useful for a number

of applications, including enhanced photoactivity, which is presently being investigated.

Acknowledgments

This research was supported by the US Department of Energy, Office of Basic Energy Sciences, Division of Materials Sciences and Engineering under Award No. DE-FG02-08ER46537.

References

[1] Flynn C E, Lee S W, Peelle B R and Belcher A M 2003 *Acta Mater.* **51** 5867
[2] Flynn C E, Mao C, Hayhurst A, Williams J L, Georgiou G, Iverson B and Belcher A M 2003 *J. Mater. Chem.* **13** 2414
[3] Vriezema D M, Comellas Aragonès M, Elemans J A, Cornelissen J J, Rowan A E and Nolte R J 2005 *Chem. Rev.* **105** 1445
[4] Douglas T and Young M 2006 *Science* **312** 873
[5] Fischlechner M and Donath E 2007 *Angew. Chem. Int. Edn* **46** 3184
[6] Uchida M, Klem M T, Flenniken M, Allen M, Varpness Z, Gillitzer E, Suci P, Young M and Douglas T 2007 *Adv. Mater.* **19** 1025
[7] Lee L A, Niu Z and Wang Q 2009 *Nano Res.* **2** 349
[8] Huang R K, Steinmetz N F, Fu C Y, Manchester M and Johnson J E 2011 *Nanomedicine* **6** 55
[9] Kang S, Lander G C, Johnson J E and Prevelige P E 2008 *ChemBioChem* **9** 514
[10] Kang S, Uchida M, O'Neil A, Li R, Prevelige P E and Douglas T 2010 *Biomacromolecules* **11** 2804
[11] Shen L, Bao N, Prevelige P E and Gupta A 2010 *J. Am. Chem. Soc.* **132** 17354
[12] Reichhardt C, Uchida M, O'Neil A, Li R, Prevelige P E and Douglas T 2011 *Chem. Commun.* **47** 6326
[13] Johnson J E 2010 *Curr. Opin. Struct. Biol.* **20** 210
[14] Prevelige P E Jr, Thomas D and King J 1988 *J. Mol. Biol.* **202** 743
[15] Wei Y, Yang J and Ying J Y 2010 *Chem. Commun.* **46** 3179
[16] Parent K N, Gilcrease E B, Casjens S R and Baker T S 2012 *Virology* **427** 177
[17] Casjens S and King J 1974 *J. Supramol. Struct.* **2** 202
[18] Prevelige P E Jr, Thomas D and King J 1988 *J. Mol. Biol.* **202** 743
[19] Bermudez H and Hathorne A P 2008 *Faraday Discuss.* **139** 327
Curtis S B, MacGillivray R T A and Dunbar W S 2011 *Biotechnol. Bioeng.* **108** 1579
[20] Fuller M T and King J 1980 *Biophys. J.* **32** 381
[21] Jiang W, Li Z, Zhang Z, Baker M L, Prevelige P E and Chiu W 2003 *Nature Struct. Biol.* **10** 131
[22] Kang S, Hawkridge A M, Johnson K L, Muddiman D C and Prevelige P E 2006 *J. Proteome Res.* **5** 370
[23] Gertsman I, Gan L, Guttman M, Lee K, Speir J A, Duda R L, Hendrix R W, Komives E A and Johnson J E 2009 *Nature* **458** 646
[24] Parent K N, Khayat R, Tu L H, Suhanovsky M M, Cortines J R, Teschke C M, Johnson J E and Baker T S 2010 *Structure* **18** 390
[25] Brewer S H, Glomm W R, Johnson M C, Knag M K and Franze S 2005 *Langmuir* **21** 9303